Corrosivity monitoring system using RFID-based sensors

Lawand, Lydia, Shiryayev, Oleg, Alhandawi, Khalil, Vahdati, Nader, Rostron, Paul

Lydia Lawand, Oleg Shiryayev, Khalil B. Alhandawi, Nader Vahdati, Paul Rostron, "Corrosivity monitoring system using RFID-based sensors," Proc. SPIE 9803, Sensors and Smart Structures Technologies for Civil, Mechanical, and Aerospace Systems 2016, 98031F (20 April 2016); doi: 10.1117/12.2218813

SPIE.

Event: SPIE Smart Structures and Materials + Nondestructive Evaluation and Health Monitoring, 2016, Las Vegas, Nevada, United States

Corrosivity monitoring system using RFID-based sensors

Lydia Lawand[a], Oleg Shiryayev[a], Khalil B. Alhandawi[a], Nader Vahdati[a], and Paul Rostron[a]

[a]3007 Dept. of Mechanical Engineering, The Petroleum Institute
PO Box 2533, Umm Al Nar, Abu Dhabi
United Arab Emirates

ABSTRACT

In the oil and gas industry, pipeline integrity is a serious concern due to the consequences of pipeline failure. External corrosion was identified as one of the main causes of pipeline failures worldwide. A solution that addresses the issue of detecting and quantifying corrosivity of environment for application to existing exposed pipelines has been developed. The proposed sensor consists of an electric circuit and a sensing array connected to the circuit. The sensing array is an assembly of strips made of a metal identical to that of the pipe, having the same length and width, but different thicknesses. The sensing array is exposed to the same environment as the pipe. As corrosion propagates in the metal strips of the array, it corrodes the metal until it finally breaks the metal strip apart resulting in a discontinuity in the circuit. The sensor circuit is energized using electromagnetic field, and its function is to indicate which strips in the array are fully corroded. Visual indication is provided to the operator via LEDs. The proposed sensor can be installed on existing pipelines without altering the pipe structure or disturbing the production process. It is passive and has low maintenance requirements. Circuit design was validated through lab experiments. Results obtained from experiments were consistent with simulation results.

Keywords: RFID technology, external corrosion, pipelines

1. INTRODUCTION

Pipeline Integrity Management System is an innovative approach that helps minimizing risk of failures, allows higher productivity, longer asset life, improved reliability, lower operation costs, and ensures compliance with the regulations.[1] Most industrial units are made of carbon steel as it has a relatively low cost and excellent mechanical properties. However, carbon steel is found to be highly corrosive, affecting the lifespan of the equipment, causing environmental pollution, and loss of resources. External corrosion is one of the major causes of hydrocarbon pipeline failures in the oil and gas industry; thus, the potential consequences of pipeline corrosion failures should not be underestimated. PHMSA (Pipeline and Hazardous Materials Safety Administration) statistics in the US have reported about 9.4% of pipeline damages between the years 1994 and 2013 due to external corrosion.[2] Moreover, the 8th EGIDG (European Gas Pipeline Incident Data Group) report has revealed that 16.1% of gas pipeline incidents in Europe between the years 2007 and 2010 were caused by corrosion problems.[3]

The key objective of this research is to come up with a solution that addresses the issue of detecting and monitoring corrosivity of environment in vicinity of existing exposed pipelines in the oil and gas industry. This will help in development of so called "corrosion maps" that will indicate locations along the pipeline that are prone to corrosion. In order for the proposed solution to be feasible and practical, it is crucial for the solution to retain the following characteristics:

- The proposed sensor should be passive, therefore it should not require constant electric power supply.
- The proposed sensor should be non-invasive, allowing its installation without altering existing pipe structure or having to terminate production in the pipe.

Further author information: (Send correspondence to Lydia Lawand)
Lydia Lawand: E-mail: lyslawand@pi.ac.ae, Telephone: +971 50 8213210
Oleg Shiryayev: E-mail: oshiryayev@pi.ac.ae, Telephone: +971 02 6075451

Sensors and Smart Structures Technologies for Civil, Mechanical, and Aerospace Systems 2016,
edited by Jerome P. Lynch, Proc. of SPIE Vol. 9803, 98031F · © 2016 SPIE
CCC code: 0277-786X/16/$18 · doi: 10.1117/12.2218813

- The proposed sensor should be able to provide real time monitoring of corrosion on existing pipes. This is desirable, but not a required characteristic.
- The proposed sensor should be economically efficient when compared to existing and conventional corrosion monitoring techniques.
- Maintenance and replacement of the proposed sensor should be relatively easy and cheap.

2. REVIEW OF LITERATURE

External corrosion of pipelines is caused by electrochemical activity occurring on the pipe surface resulting in an oxide layer build up. The presence of water and a conductive material is necessary for corrosion to occur resulting in the development of anodic and cathodic sites. Local macro-environmental parameters and external environmental factors have an impact on external corrosion.[4] Pulsed eddy current (PEC),[5] radiography techniques, Fiber Bragg Grating (FBG)[6] hoop-strain sensors and Magnetic Flux Leakage (MFL)[7] are conventional nondestructive testing tools that allow inspection, testing, or evaluation of components for corrosion damage without destroying the functionality and structural integrity of the part. However, most of these techniques require relatively large input power, are highly sensitive to protruding parts and sensor arrangement as the spatial resolution and sensor sensitivity decrease as the standoff distance increases. In addition, optical techniques such as FBG sensors are fragile, highly sensitive to temperature and provide limited information about corrosion rate and material loss as it is computationally complex to convert features of optical signals to corrosion damage information.[6] Implementation of regular inspections or instrumentation of entire pipelines using these techniques can be rather time consuming and costly, given the size of the pipeline networks. Hence, it is proposed to develop a corrosivity sensor that will allow to determine which segments of the pipeline are more prone to corrosion than others. This information is very valuable for developing of a cost-effective asset integrity management program.

After evaluating a few options, it was decided to focus on the concept that utilizes RFID technology because it allows to retain most of characteristics mentioned in section 1. Various RFID-based sensors exist that monitor corrosion using a parasitic element that interacts with the environment, changing its characteristics and resulting in a change in the magnitude of electromagnetic response between the sensor's inductive element and the antenna of the reader.[8] Another structural health sensor detects moisture to monitor corrosion in various aircraft structures.[9] The sensor consists of wires coated with soluble shields. Once exposed to moisture, the shields will dissolve, bringing the two conductive wires in contact, and forming a short circuit, which terminates communication with the RFID chip. Passive wireless corrosion sensor includes corrosion sensitive link that interposes the circuit and the antenna.[10] When exposed to the surrounding environment, the corrosion sensitive link will get corroded, breaking the circuit, hence the sensor will not be able to send a response signal back to the transceiver. The above mentioned sensors either require a constant power supply, or rely on transmission of signals from the sensing circuit back to the interrogating equipment. Reliability of the data stream will be relatively low because the sensor will be located in very close vicinity to the metal pipe. It was decided to develop a sensor the reading of which can be easily interpreted by visual observation.

3. METHODOLOGY

This section will present the design methodology used to test the feasibility of proposed corrosion sensor design. The proposed sensor consists of strips of a metal identical to that of the pipe having the same length and width, but different thicknesses with each connected to an LED in the transponder circuit. As corrosion propagates in the metal strips, it eats the metal away until it finally breaks the metal strip apart resulting in a discontinuity in the circuit. The discontinuity in the circuit will switch off the corresponding LED so that it will not light up when the circuit is energized. The thinnest strip is expected to fail first. Once no signal can be sensed from the circuit containing the strip with the largest thickness, it can be concluded that critical corrosion exists in that region of the pipeline and action must be taken in order to prevent any accidents.

Fig. 1 shows a schematic of the proposed sensor design. Bringing the tag and reader antenna close enough to each other, an alternating electromagnetic field will be produced. The alternating field then induces a voltage on the tags antenna coil. The tag then uses this energy to power the the circuit, thus lighting up the LEDs.

Therefore, when any of the LEDs fails to light up, it can be concluded that corrosion has eaten away most of the metal strip connected to that LED. Unlike the RFID-based sensors that exist in literature, the proposed sensor does not rely on data exchange between the reader and the tag, hence improving reliability of interrogation. It was decided to utilize low frequency RFID because it is less prone to interference issue when operated near metals and liquids. The proposed sensor can be used for corrosion mapping, while having lower power requirement than conventional sensors as no computations are performed on the sensor.

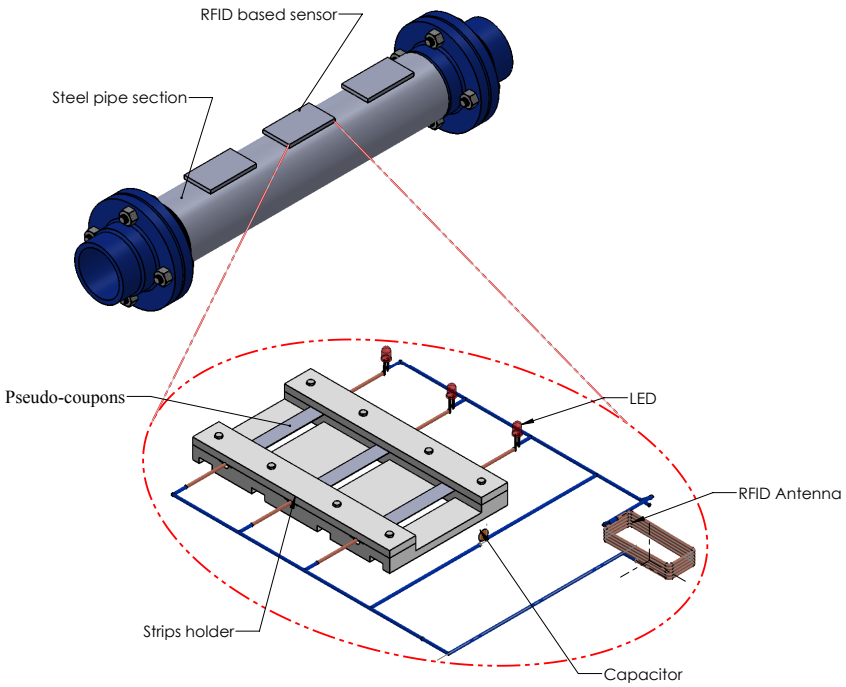

Figure 1. Schematic of the proposed sensor design.

The proposed sensor is similar to an RFID tag consisting of an antenna attached to a substrate and connected to four metal strips with various thicknesses, which will be used as the sensing elements. Metal strips used in the proposed sensor are selected to be of the same material as that of the pipe so that they closely represent the real world conditions of the pipe. The thickness dimensions of the metal strips are determined by studying the corrosion rate of steel.

The corrosion rate of steel exposed to different environments provided by the ISO 9323 standard was used to illustrate the reduction in steel thickness (m) at different exposure times.[11] Our goal is to propose a sensor design that is capable of giving information about the location and degree of corrosion within approximately 30 days. The graph in Fig. 2 shows of the range of required thickness dimensions for mild steel.

Rectangular shaped sensing elements will be used in the sensor as they have a large surface area compared to wire shaped elements, allowing corrosion to develop on the surface. One advantage that rod or wire shaped coupons have over rectangular ones is that they do not require orientation in the flow, as their cylindrical shape prevents edge effects from occurring. Metal strips serving as the sensing elements in the proposed corrosion sensor will not be pre-stressed as there is almost negligible risk of stress corrosion cracking in the environments the sensor will be used in. Based on the desired thickness values shown in Fig. 2, metal strips used in the proposed corrosion sensor should be manufactured using nanofabrication processes.

In order to achieve the objective of this research and come up with a feasible corrosion sensor that could be used on oil and gas pipes, modeling and experiments were conducted on the proposed sensor concept. A model

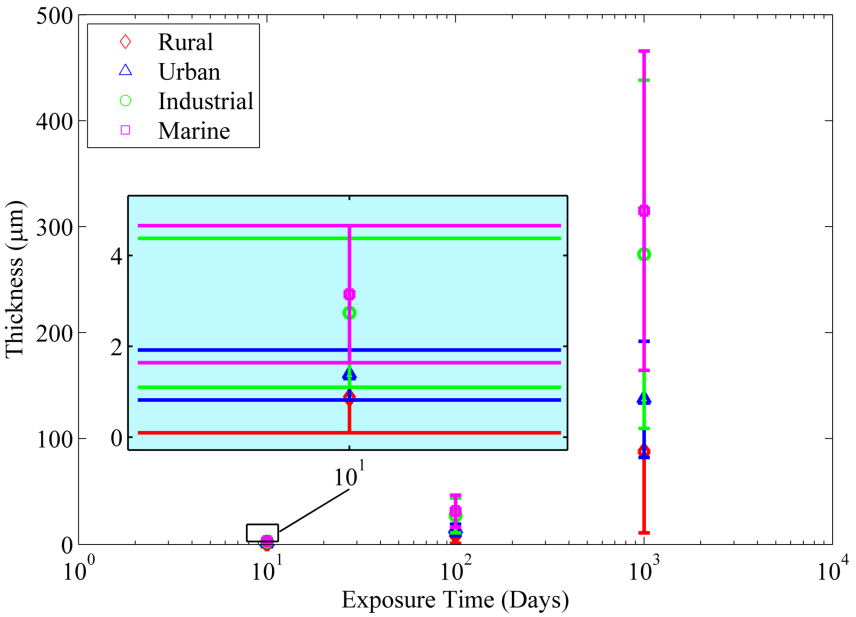

Figure 2. Loss of thickness of steel strips at different exposure times for different environments[11] .

of both the tag and reader circuits was created and simulations were run to test the sensor's performance as shown in the next chapter. Experiments were then conducted to validate simulation results. Results obtained at different read ranges are also illustrated and discussed.

4. LINEAR CIRCUIT ANALYSIS

A model of both the reader and the tag circuit was developed and implemented in Simulink in order to facilitate sensor circuit design and ensure its functionality. However, since the LEDs present in the tag circuit will cause the electric circuit being modeled to be non-linear, a simplified linear electric circuit consisting of resistors instead of LEDs was created and simulated prior to the actual circuit. Equivalent transponder and sensor circuits were then built in the lab to be used to validate the numerical model that was created. The transponder unit was custom designed to be able to monitor analogue signal from the tag coil. The transponder circuit was powered using a function generator and the sensor circuit was powered by mutual coupling between the antennas. A digital multimeter was used to measure the inductance of the antennas, while the corresponding capacitances were calculated using Equation (1). A capacitor is needed in the tag circuit to help form a tuned LC circuit.

$$L = \frac{1}{4\pi^2 c f^2} \tag{1}$$

where: L = inductance (H), c = capacitance (F), and f = frequency (Hz).

Fig. 3 shows a schematic diagram of the linear circuit with resistors that was initially modeled. The voltage induced in the tag inductor loop is governed by Faradays law of induction, which states that a changing magnetic flux generates an electromotive force (voltage) in the conductor. In its general form Faradays law is written as:

$$u_1 = \oint Eds = -N\frac{d\Psi(t)}{dt} \tag{2}$$

The efficiency of the equivalent circuit in Fig. 3 is greatly improved by the use of a capacitor C_2 connected in parallel to the tag coil L_2 to form a resonant circuit with a resonant frequency corresponding to the carrier frequency. The resonant frequency f_r can be calculated using the Thomson equation:

$$f_r = \frac{1}{2\pi\sqrt{L_2.C_2}} \tag{3}$$

where: L = inductance (H), c = capacitance (F), and f = frequency (Hz). In this work we considered 125 kHz frequency typically used in low frequency RFID systems.

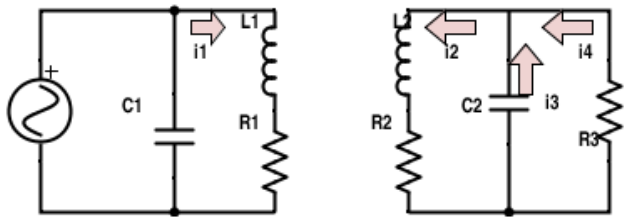

Figure 3. Schematic diagram of the circuit with a resistor.

The following equations describe the numerical model of the linear circuit:

$$\frac{di_1}{dt} = \frac{v_i}{L_1} + \frac{M}{L_1}\frac{di_2}{dt} - \frac{R_1 i_1}{L_1} \tag{4}$$

$$\frac{di_2}{dt} = \frac{M}{L_2}\frac{di_1}{dt} - \frac{R_2 i_2}{L_2} - \frac{1}{C_2 L_2}\int i_3 dt \tag{5}$$

$$i_4 = \frac{M}{R_3}\frac{di_1}{dt} - \frac{L_2}{R_3}\frac{di_2}{dt} - \frac{R_2}{R_3} i_2 \tag{6}$$

$$M\frac{di_1}{dt} - L_2\frac{di_2}{dt} - R_2 i_2 - R_3 i_4 = 0 \tag{7}$$

$$M\frac{di_1}{dt} - L_2\frac{di_2}{dt} - R_2 i_2 - \frac{1}{C_2}\int i_3 dt = 0 \tag{8}$$

where v_i is the voltage signal at the voltage source; i_1, i_2, i_3 and i_4 are currents across different circuit components as shown in Figure 3; L_1 and L_2 are inductance values of the corresponding inductors; C_2 is the capacitance value of the capacitor shown in Figure 3; R_1 and R_2 are resistance values of the inductors shown in Figure 3; R_3 is the resistance value of the resistor used in the model shown in Figure 3; and M is mutual coupling coefficient that is calculated using Equation (9).[12]

$$M = -N_2\frac{N_1\mu l_1 l_2}{\pi}\left(\frac{1}{(l_2^2+r^2)\sqrt{l_1^2+l_2^2+r^2}} + \frac{1}{(l_1^2+r^2)\sqrt{l_1^2+l_2^2}+r^2}\right)a_1 b_1 \tag{9}$$

Here, N_1 is the number of turns in transmit (reader) coil, N_2 is the number of turns in coupling (tag) coil, μ is the permeability of free space = $4\pi \times 10^{-7}$, l_1 and l_2 are half the length and width of the reader coil respectively, a_1 and b_1 are length and width of the coupling (tag) coil respectively and r is the distance between transmit coil and coupling coil (read distance).

4.1 Experimental Setup

In order to check the accuracy of simulation results with respect to the real system, an experiment was performed. Fig. 4 shows the experimental setup used to conduct this experiment. A function generator was used to supply 5V sine wave at 125 kHz to the reader circuit.

Figs. 5 and 6 illustrate good agreement between numerical prediction and experimental data. One can observe the decrease in the amplitude of induced voltage as the distance between the two antennas increases. Hence, the basis was formed to develop the nonlinear model containing the LEDs.

5. NONLINEAR CIRCUIT ANALYSIS

After analyzing the linear circuit, a more accurate model of the actual sensor circuit was created which consists of three LEDs in parallel, with each of them connected in series to an 11 Ω resistor. Fig. 7 shows a schematic

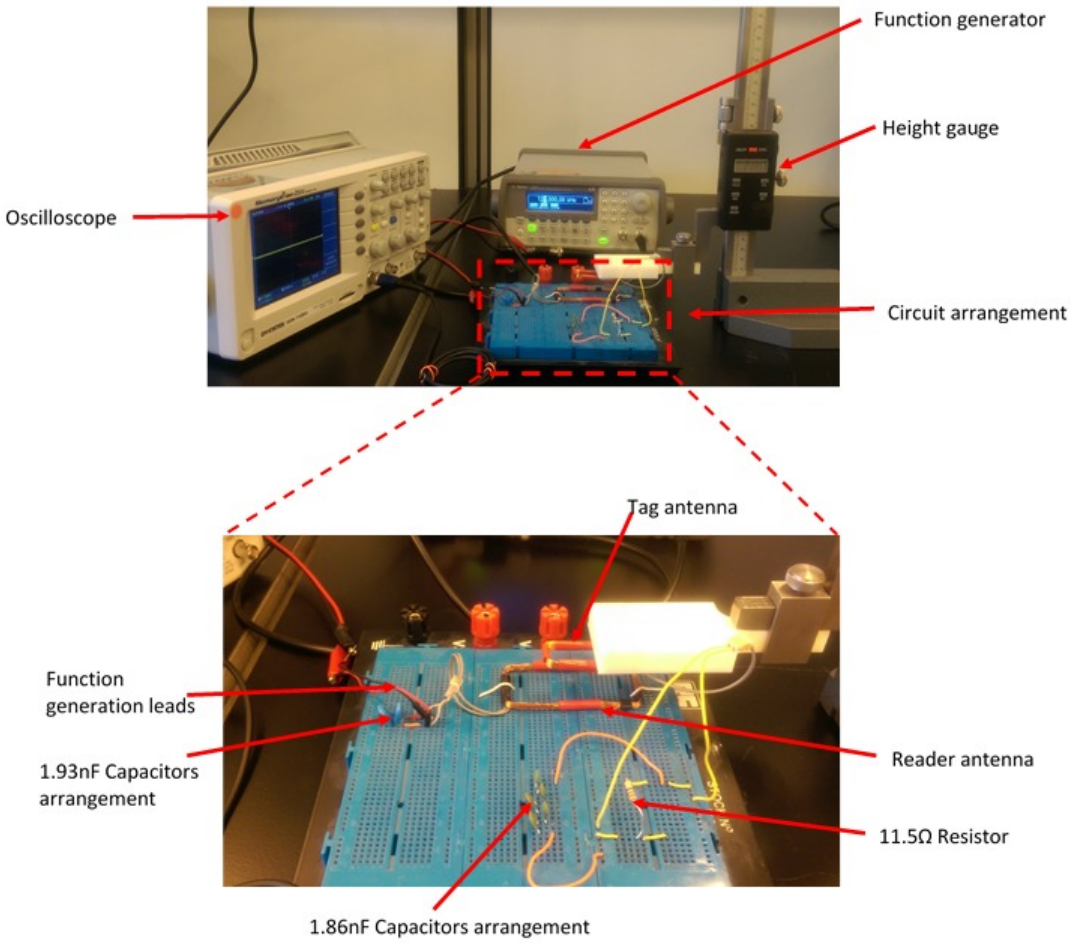

Figure 4. Experimental setup of the linear circuit (with resistor).

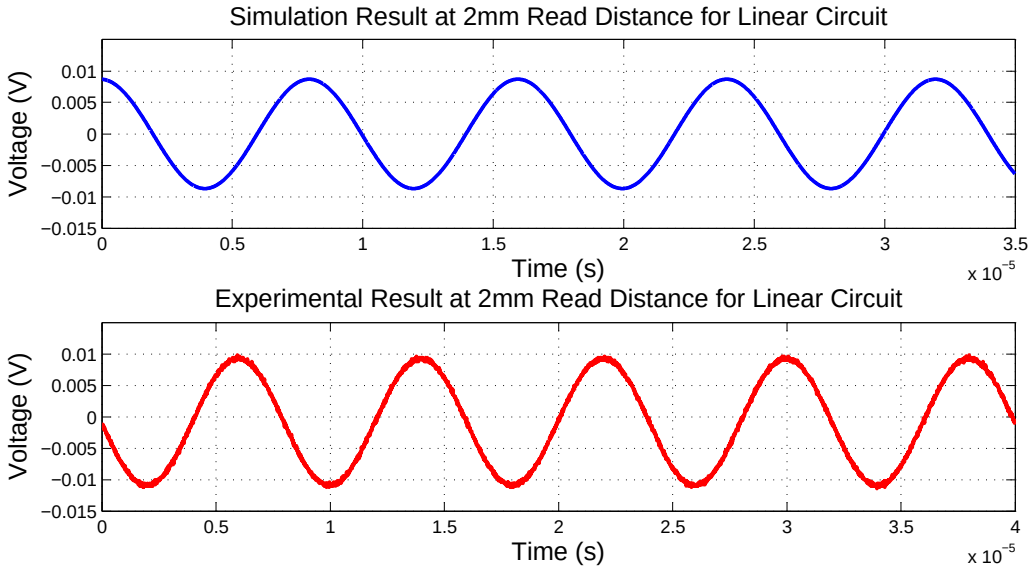

Figure 5. Comparison of experimental and simulation results at 2 mm distance between antennas.

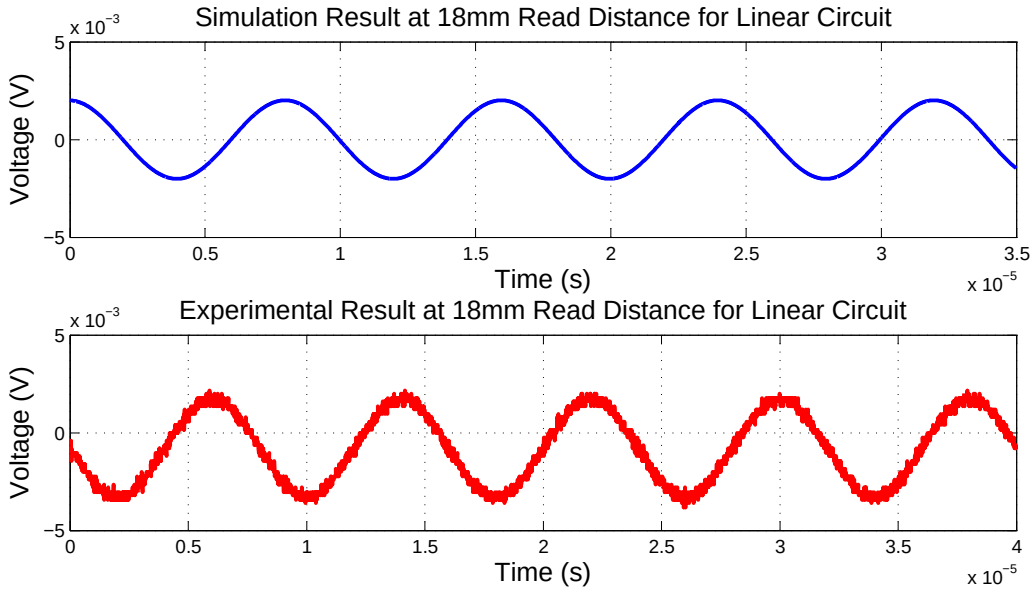

Figure 6. Comparison of experimental and simulation results at 18 mm distance between antennas.

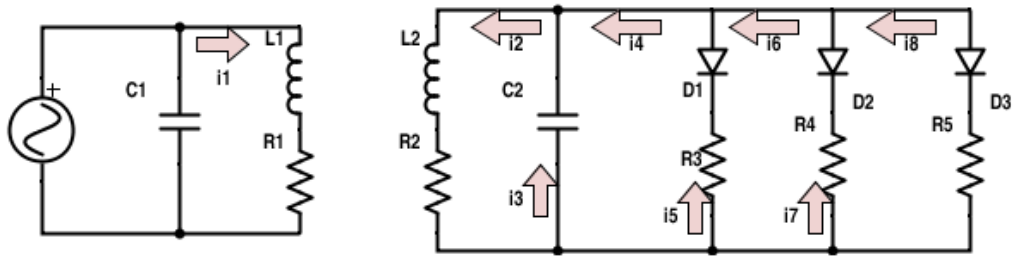

Figure 7. Schematic diagram of a circuit with 3 LEDs.

diagram of the circuit containing 3 LEDs. Antennas are represented by equivalent inductors and resistors, with both mutual and self-inductances taken into consideration. Green (3 mm) diffused LED lamps were used in the experimental setup. In order to create a reliable model that closely reflects the components used in the experiment, the characteristic curve of green diffused LED lamps showing the relation between the forward current and voltage through the LED lamps was inputted into the Simulink model.[13] The curve was obtained from the datasheet provided by the manufacturer. Below are the equations that represent the nonlinear circuit

with 3 LEDs.

$$\frac{di_1}{dt} = \frac{v_i}{L_1} + \frac{M}{L_1}\frac{di_2}{dt} - \frac{R_1 i_1}{L_1} \tag{10}$$

$$\frac{di_2}{dt} = \frac{M}{L_2}\frac{di_1}{dt} - \frac{R_2 i_2}{L_2} - \frac{1}{C_2 L_2}\int i_3 dt \tag{11}$$

$$v_{1LED} = M\frac{di_1}{dt} - L_2\frac{di_2}{dt} - R_2 i_2 - R_3 i_5 \tag{12}$$

$$v_{2LED} = M\frac{di_1}{dt} - L_2\frac{di_2}{dt} - R_2 i_2 - R_4 i_7 \tag{13}$$

$$v_{3LED} = M\frac{di_1}{dt} - L_2\frac{di_2}{dt} - R_2 i_2 - R_5 i_8 \tag{14}$$

$$i_8 + i_7 = i_6 \tag{15}$$

$$i_6 + i_5 = i_4 \tag{16}$$

$$i_4 + i_3 = i_2 \tag{17}$$

5.1 Experimental Setup

After running the simulation, results obtained were validated by experiments. Fig. 8 shows the experimental setup of a circuit with three LEDs and resistors that is equivalent to the circuit that will be used in the proposed corrosion sensor.

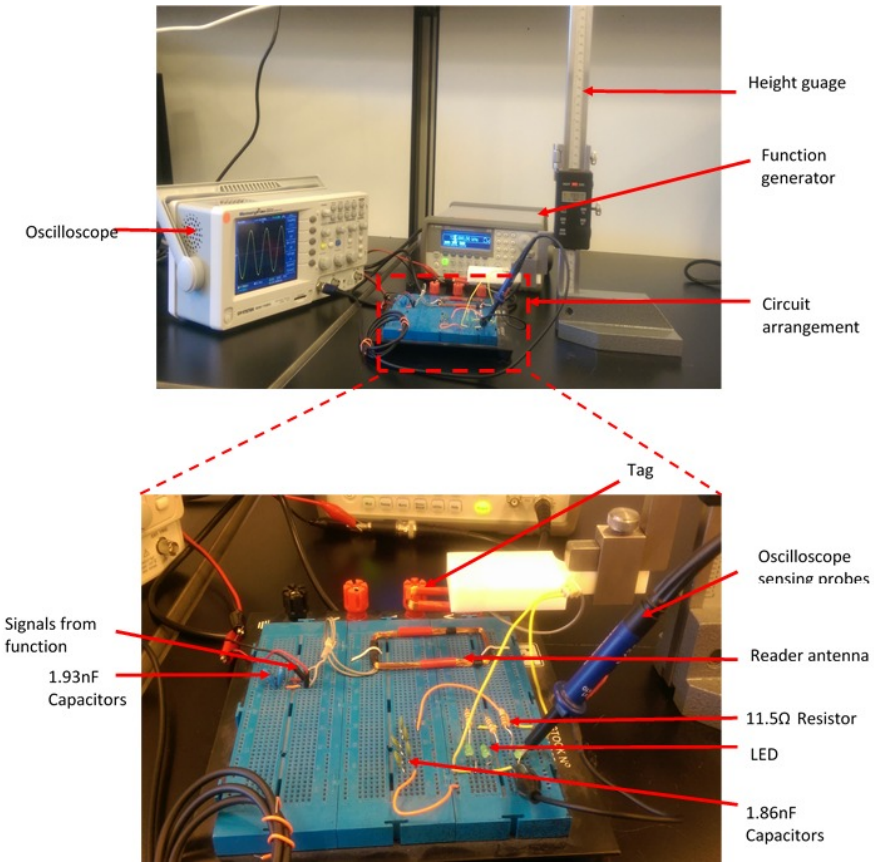

Figure 8. Experimental setup of circuit with 3 LEDs.

5.2 Comparison of Results

Clipping of the voltage signal was observed in both experimental and simulation results for distances between antennas up to 8 mm. Clipping depends mainly on the amplitude of the input signal supplied by the function generator and parameters of the diodes used. It occurs whenever the voltage across the diode is greater than the diode's threshold voltage, so the diode starts conducting the current and emitting light. On the other hand, if the voltage across the diode is less than threshold voltage, it will not conduct and will not emit visible light. This situation is shown in Fig. 10 for the 26 mm distance case.

The orientation of the diode in the circuit will also determine whether there will be a positive or negative shift on the y-axis. The circuit modeled is a positive peak clipper circuit. A good agreement between the results can be observed with both waves from the experiment and simulation having the same frequency. The amplitude of the signal decreased as the distance between the two antennas increased. For both experimental and simulation data, both antennas are located in parallel planes directly opposite to one another, and displacement of the reader antenna is assumed to occur only in the z direction.

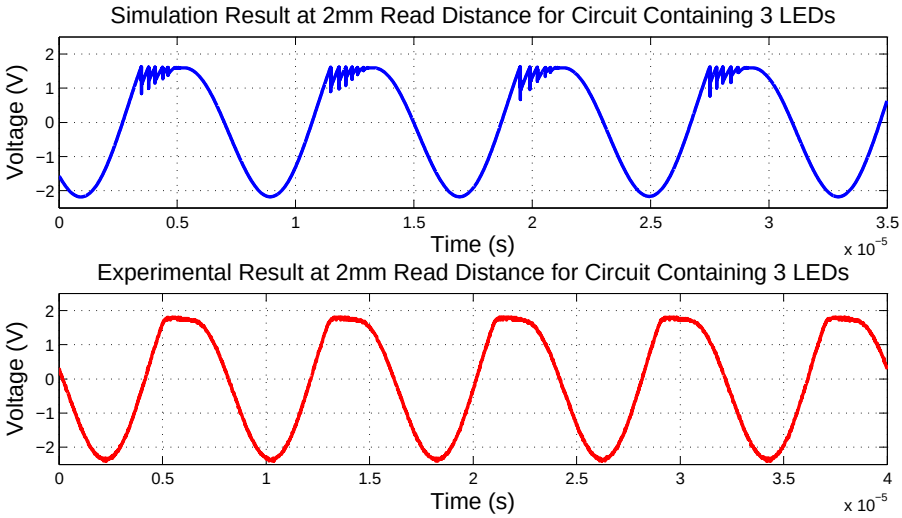

Figure 9. Comparison of both experimental and simulation results at 2 mm read distance for a circuit containing 3 LEDs.

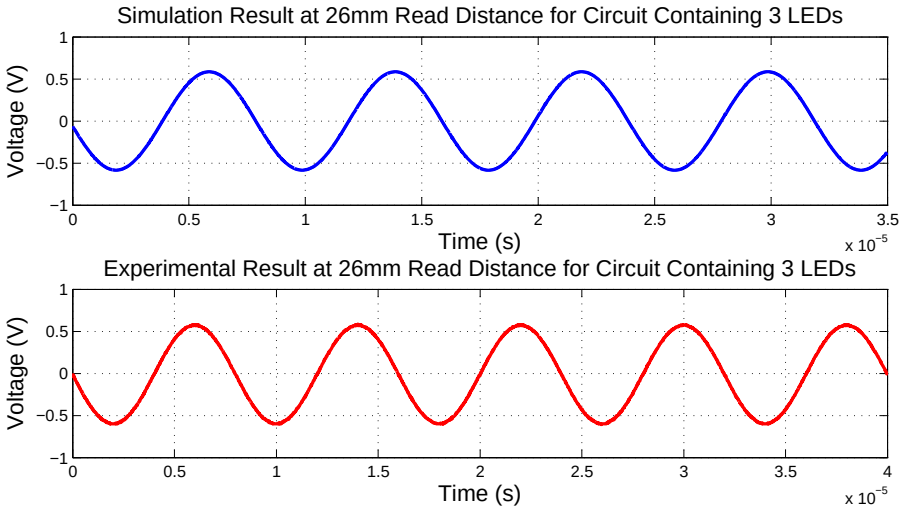

Figure 10. Comparison of both experimental and simulation results at 26 mm read distance for a circuit containing 3 LEDs.

5.3 Repeatability of results

Another aspect of this study was to evaluate the repeatability and variability of results obtained experimentally. Ten measurements were conducted at each distance value. Results at 0 mm, 2 mm, and 4 mm distance values are shown in Fig. 11 for illustration purposes. Results obtained in all cases were further analyzed by calculating the mean and standard deviation of positive and negative peak values of the measured waveforms to check the repeatability of conducted experiments. It was concluded that the experiment has a relatively high repeatability as the largest calculated standard deviation value was only 0.03 V when the mean upper and lower limiting voltage values were on the order of 1.4-1.5 V.

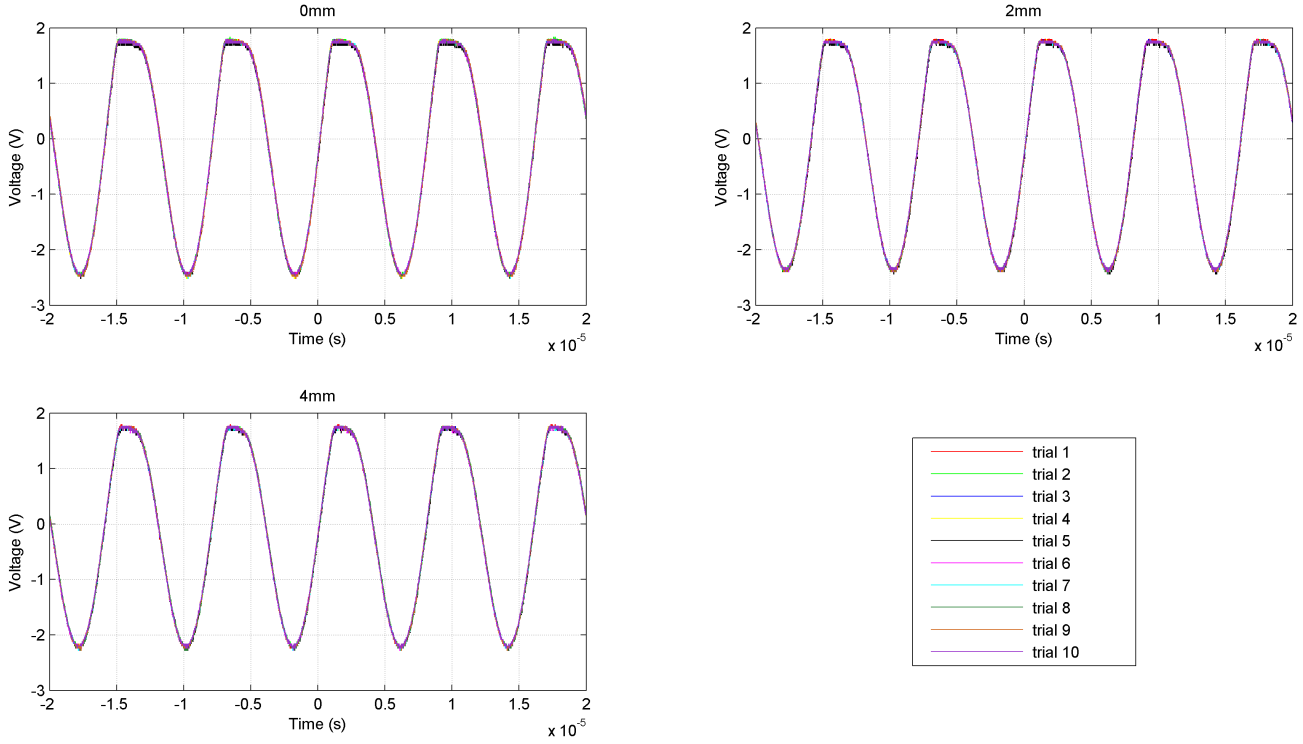

Figure 11. Repeatability test results at 0 mm, 2 mm, and 4 mm read distances.

6. CONCLUSIONS

This paper presents initial steps in addressing the challenge of developing an inexpensive and reliable corrosivity sensor to be used for monitoring the environment in vicinity of over the ground pipelines. This sensor will help in development of so called "corrosion maps" that will indicate locations along the pipeline that are prone to corrosion. Corrosion maps are important for the development of cost effective asset integrity management strategies.

The proposed sensor consists of two main parts: the sensing array and the interrogation circuit. The sensing array is composed of an assembly of metal strips interconnected with the interrogating circuit. The interrogator circuit is a resonant circuit tuned to the frequency of the external RF signal. The circuit is energized by the RF energy emitted from the device carried by the operator who visually examines the LEDs in the circuit to determine the level of corrosion that has taken place on the sensing array. Low frequency RFID technology operating at 125 kHz was chosen as the basis for the design due to it being less prone to interference when operated near metals and liquids. The proposed sensor addresses most of the design characteristics set forth by the potential end users: it is passive, non-invasive, and safe to be used near oil and gas pipelines.

This work describes the model that was developed in order to allow efficient design of the sensing array and the corresponding circuit. Good agreement between simulation and experimental results was observed with the experiment being highly repeatable. Different sensing strip sizes can be studied by altering the values of resistors used in the simulation and observing results. Moreover, the effect of various circuit components on the functioning of the sensor can be tested using this model. The next step in this work is to develop and build a physical prototype and test it in a highly corrosive environment. In addition, the issue of relatively short sensor actuation range must be addressed. The actuation distance can be increased by the use of more powerful transmitter and through careful optimization of resonant circuit parameters.

Acknowledgments

The authors would like to acknowledge the support provided by the Petroleum Institute and the Abu Dhabi Company for Onshore Petroleum Operations (ADCO).

REFERENCES

[1] Hopkins, P., [*The Structural Integrity Of Oil And Gas Transmission Pipelines*], Elsevier Publishers, UK (2002).

[2] [*Significant Pipeline Incidents By Cause*], US Department of Transportation, Washington, DC (2014).

[3] [*8th Report of the European Gas Pipeline Incident Data Group*], European Gas Pipeline Incident Data Group (EGIG) (2011).

[4] Marney, D. and Cole, I., "The science of pipe corrosion: A review of the literature on the corrosion of ferrous metals in soils," *Corrosion Science* **56**, 5–16 (2011).

[5] Sophian, A., Tian, G., Taylor, D., and Rudlin, J., "Design of a pulsed eddy current sensor for detection of defects in aircraft lap-joints," *Sensors and Actuators* **101**, 92–98 (2002).

[6] Jia, Z., Li, H., Song, G., and Ren, L., "Design and experimental study on FBG hoop-strain sensor in pipeline monitoring," *Optical Fiber Technology* **20**(1), 15–23 (2014).

[7] Hay, B. and Smith, J., "Magnetic flux leakage inspection tool for pipelines," *US Patent US 6023986 A* (Feb. 2000).

[8] Friedersdorf, F., Bopp, C., and Wavering, T., "Wireless corrosion sensor," *US Patent US 8085165 B2* (Dec. 2011).

[9] Kearns, J., Bommer, J., Fay, M., and Pena, G., "Transmission line moisture sensor," *US Patent US 20100182023 A1* (2010).

[10] Apblett, A. and Materer, N., "Passive wireless corrosion sensor," *US Patent US 20090058427 A1* (Mar. 2009).

[11] Moller, P., "Evaluation of atmospheric corrosion on electroplated zinc and zinc-nickel coatings by electrical resistance (ER) monitoring," *NASF Surface Technology White Papers* **78**(5), 1–10 (2014).

[12] Tang, X., Yang, J., Ao, J., and He, Y., "The principle and simulation of magnetic coupling for rectangular coil in mobile payment system," in [*Proceedings of 2011 International Conference on Wireless Communications and Signal Processing*], IEEE (2011). doi: 10.1109/WCSP.2011.6096868.

[13] "HLMP–1301,HLMP–1401, HLMP–1503, HLMP–K401, HLMP–K600, T–1(3mm) Diffused LED Lamps datasheet." http://docs.avagotech.com/docs/AV02-1555EN, Accessed: 20-06-2015.